HBT RADII OF CHARGED PIONS WITH SHEAR VISCOUS TRANSPORT DYNAMICS SIMULATIONS IN THE AMPT MODEL

Yao Zhang

School of Energy and Mechanical Engineering
Jiangxi University of Science and Technology
Nanchang 330013, China

Received 24 October 2024, accepted 21 December 2024, published online 14 January 2025

We utilized the AMPT model to simulate the shear viscous transport dynamics of parton matter with varying specific shear viscosity and phase-transition temperatures and investigate the effect on the HBT radii of charged pions at the $\sqrt{s_{NN}} = 200$ GeV Au+Au collisions. The emission-source size is sensitive to the shear viscosity of parton matter, thus, increasing the shear viscosity to entropy density ratio will reduce the HBT radii. The phase-transition temperature can regulate the evolution duration of the parton and hadron phases. Raising the phase-transition temperature shortens the evolution time of the partonic phase and extends the evolution time of the hadronic phase, resulting in an increase in the total system evolution time. A prolonged hadronic-phase evolution weakens the dependence of the transverse HBT radii on transverse mass and increases the evolution time scale.

DOI:10.5506/APhysPolB.56.1-A1

1. Introduction

Exploring the dynamics and properties of the quark–gluon plasma produced at the Relativistic Heavy Ion Collider (RHIC) and the Large Hadron Collider (LHC) is a primary goal of relativistic heavy-ion collision research. The strongly coupled deconfinement QGP produced in nuclear–nuclear collisions exhibits rapid hydrodynamic expansion similar to that of an almost perfect fluid [1–7]. Its temperature-dependent viscosity coefficient can be precisely estimated using the Bayesian parameter estimation method, with the shear viscosity coefficient approaching the KSS bound near the phase-transition temperature [8–10]. Understanding the spatiotemporal evolution of the full system is essential for investigating the characteristics of QGP.

However, due to the complexity of the collision system, experimental observables based on models are frequently employed to study the system properties. A multi-phase transport model (AMPT), which includes partonic- and hadronic-transport processes based on non-equilibration transport dynamics, has been widely applied in heavy-ion collision studies [11–15]. The shear viscous transport dynamics simulation of parton matter enables the quantitative study of shear viscosity and phase-transition temperature, which are closely related to system evolution within the AMPT model [16–18].

The measurements of the space-time distribution at kinetic freeze-out can provide constraints on the system evolution and the HBT interferometry, as an important observable can be used to measure the spatial and temporal scales of systems, and detect the space-time substructure and momentum correlations of the freeze-out configuration in heavy-ion collisions [19–24]. With the shear viscous transport dynamics simulation by the Chapman–Enskog (CE) methods, we simulate Au+Au collisions at $\sqrt{s_{NN}} = 200$ GeV in the AMPT model, and study the influences of different specific shear viscosity and phase-transition temperatures on the charged pion HBT radii and evolution time scale. In Section 2, we implement the shear viscous transport dynamics simulations of parton matter in the AMPT model. In Section 3, the charged pion HBT radii and evolution time scale are discussed. We conclude in Section 4.

2. Shear viscous simulation of partonic-transport dynamics

The shear viscosity in the transport process of parton matter can be numerically expressed as functions of finite temperature and scattering cross section, despite the differences in numerical estimates obtained from different analytical methods based on kinetic theory [25]. The AMPT model is a hybrid model incorporating partonic- and hadronic-transport processes to generate heavy-ion collision events, with parton interactions based on the two-body forward-angle scattering process of the ZPC cascade model [26]. In the CE method applicable to anisotropic scattering, the shear viscosity can be expressed as

$$\eta = \frac{4T}{5\sigma_p\, g(w)}\,, \tag{1}$$

where σ_p is the partonic-scattering cross section, $g(w)$ is the thermal average of $h(a) = 4a(1+a)[(1+2a)\ln(1+\frac{1}{a})-2]$ and can be approximated as [25, 27]

$$g(w) \approx h\left(\frac{w^2}{v^2}\right)\,, \tag{2}$$

with $w = \mu/T$, μ being the screening mass and $v = 11.31–4.847\exp(-0.1378\, w^{0.7338})$. At temperature T, the parton matter of massless three-flavor quarks is assumed, the shear viscosity-to-entropy density ratio is [18]

$$\eta/s \approx \frac{2\pi w^2}{45 g_{\mathrm{B}} \alpha_{\mathrm{s}}^2 g(w)}\,, \tag{3}$$

where $g_{\mathrm{B}} = 52$ when using Boltzmann distribution and α_{s} is the QCD coupling constant.

The critical aspect of simulating the shear viscous transport dynamics simulation of parton matter in the AMPT model is the adjustment of μ/T during the system evolution for a fixed α_{s}, enabling quantitative control of the parameterized $\eta/s(T)$ in parton interactions. Compared to the easily adjustable input parameter μ, which is directly related to the partonic-scattering cross section, $\sigma_p \approx 9\pi\alpha_{\mathrm{s}}^2/(2\mu^2)$, it is more important to obtain the spatiotemporal distribution of the parton phase temperature. The temperature distribution can be estimated using partonic-energy density under the Boltzmann distribution. In a single event, due to the small number of partons in a cell, the statistical nature of the energy density estimated by averaging the parton energy in the volume element is insufficient for extracting the temperature distribution. Hence, we use the Gaussian smearing approximation to obtain the energy density distribution by smearing each pointlike parton with a three-dimensional Gaussian distribution of its total energy. The distribution function of the parton phase temperature at evolution time t is given as

$$T(x,y,z) = \left\{ \frac{\pi^2}{3 g_{\mathrm{B}}} \sum N_i \exp\left[-\frac{(x-x_i)^2 + (y-y_i)^2 + (z-z_i)^2}{2\sigma_i^2} \right] \right\}^{\frac{1}{4}}\,, \tag{4}$$

where $N_i = (\frac{1}{2\pi})^{\frac{3}{2}} \frac{1}{\sigma_i^3} E_i$ provides the proper normalisation, (x_i, y_i, z_i), σ_i, and E_i are the position vector, Gaussian width, and energy of parton i. A continuous and consistent temperature distribution can be obtained by the Gaussian smearing approximation, which contains the spatial dependence and fluctuations of parton matter. By utilizing the temperature distribution during the evolution of parton matter, quantitative control of parameterized η/s in the model can be achieved by adjusting μ which equates to altering σ_p in two-body scattering processes. To prevent excessively long and unreasonable parton evolution times, when the effective temperature of the cell is below the phase-transition temperature T_{tr}, partons are unable to scatter in that cell and prepare for hadronization.

3. HBT radii and evolution time scale of charged pions

The shear viscous transport dynamics simulation can generate specific parameterized shear viscosity η/s and phase-transition temperature T_{tr}

of the heavy-ion collision events in the AMPT model, enabling the study of the effects of η/s and $T_{\rm tr}$ on system evolution, and measured observables within non-equilibrium transport dynamics. The parameters of the Lund string fragmentation $a_{\rm L} = 0.55$, $b_{\rm L} = 0.2$ GeV^{-2}, and the coupling constant $\alpha_{\rm s} = 0.33$ are chosen for Au+Au collisions at $\sqrt{s_{NN}} = 200$ GeV in the model.

The two-pion HBT correlation function, which is calculated by the Correlation After Burner program without the final-state interactions, can be fitted by the Bertsch–Pratt parametrization in the 'out–side–long' coordinate system [28, 29]

$$C(\boldsymbol{q}) = 1 + \lambda \exp\left(-q_{\rm o}^2 R_{\rm o}^2 - q_{\rm s}^2 R_{\rm s}^2 - q_{\rm l}^2 R_{\rm l}^2\right) , \tag{5}$$

where $q_{\rm o}$, $q_{\rm s}$, $q_{\rm l}$ are three components of the relative momentum difference $\boldsymbol{q} = \boldsymbol{p_1} - \boldsymbol{p_2}$ of a pair of pions. By fitting the correlation function, one can obtain size parameters $R_{\rm o}$, $R_{\rm s}$, and $R_{\rm l}$ which are so-called HBT radii.

Figures 1 and 2 show the charged pion HBT radii $R_{\rm o}$, $R_{\rm s}$, $R_{\rm l}$, and the $R_{\rm o}/R_{\rm s}$ ratio as a function of the average transverse mass for Au+Au collisions at $\sqrt{s_{NN}} = 200$ GeV in 0–10% centrality with $\eta/s = 0.08$ and $\eta/s = 0.16$, respectively, compared to PHENIX data. It can be seen from the figures that for constant shear viscosity, the phase-transition temperature has a significant impact on the variation of HBT radius with transverse mass $m_{\rm T}$, and the impact varies for HBT radius in different directions and

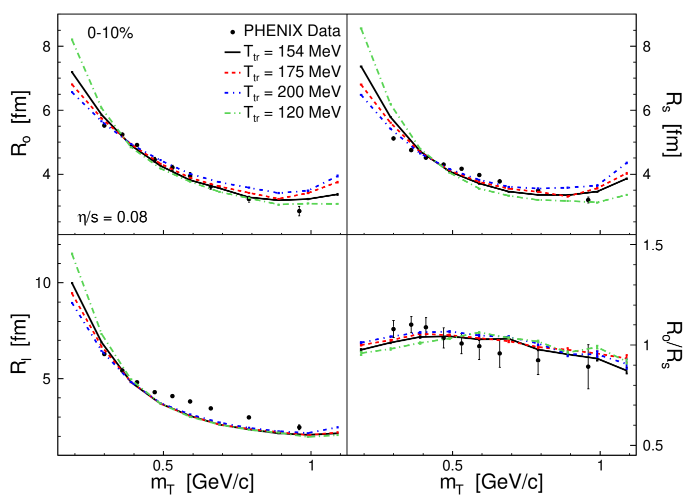

Fig. 1. HBT radii $R_{\rm o}$, $R_{\rm s}$, $R_{\rm l}$, and the $R_{\rm o}/R_{\rm s}$ ratio of charged pions varies with average transverse mass for Au+Au collisions at $\sqrt{s_{NN}} = 200$ GeV with $\eta/s = 0.08$ in 0–10% centrality compared to experimental data from the PHENIX Collaboration [22].

across different transverse mass ranges. With the same shear viscosity, the transverse mass dependence of the HBT radius weakens as the temperature increases. In the small transverse-mass range, the higher $T_{\rm tr}$, the smaller the corresponding left initial HBT radius, but higher shear viscosity will reduce the differences between the radii. In the higher transverse mass range, $R_{\rm l}$ is almost unaffected by changes in $T_{\rm tr}$, whereas $R_{\rm o}$ and $R_{\rm s}$ are increasingly affected by temperature as the transverse mass increases. $R_{\rm o}$ and $R_{\rm s}$ in the large-$m_{\rm T}$ range increases with the rise in $T_{\rm tr}$, and higher viscosity will enhance the impact on $R_{\rm o}$ compared to $R_{\rm s}$.

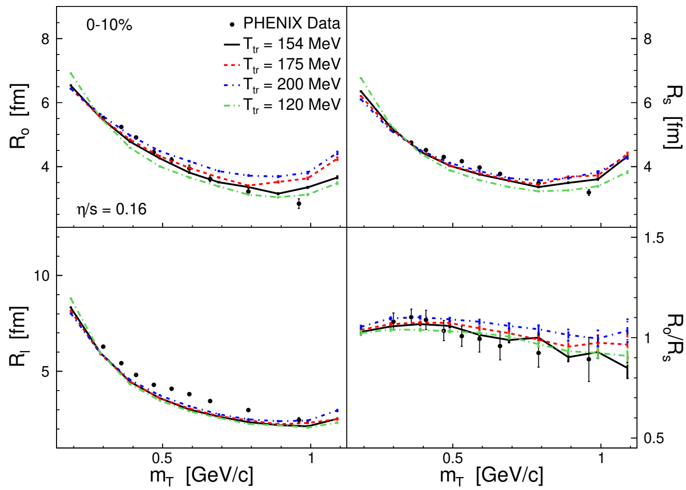

Fig. 2. The same as Fig. 1 but with $\eta/s = 0.16$.

Figure 3 shows the charged pion HBT radii as a function of the average transverse mass for Au+Au collisions with various η/s at the phase-transition temperature $T_{\rm tr} = 154$ MeV. Similar to the effect of phase-transition temperature on the HBT radius, shear viscosity also reduces the dependence of HBT radius on transverse mass, but the sensitivity of radii in different directions to η/s and $T_{\rm tr}$ varies. $R_{\rm l}$, which is less affected by $T_{\rm tr}$, is sensitive to changes in parton phase η/s, while the impact on $R_{\rm o}$ is relatively reduced. Compared to the higher $T_{\rm tr}$ resulting in smaller radii only in the small-$m_{\rm T}$ range, the influence range of η/s on the reduction of radii has significantly expanded and, as shear viscosity increases, its impact on HBT radius gradually diminishes.

Considering that pions from resonance decays can affect the HBT radius, especially in the small transverse-mass range, to distinguish whether the impact of phase-transition temperature and shear viscosity on the HBT radius originates from the source function of pions from resonance decays, we disabled the decay of ω mesons in the hadronic-transport process in the

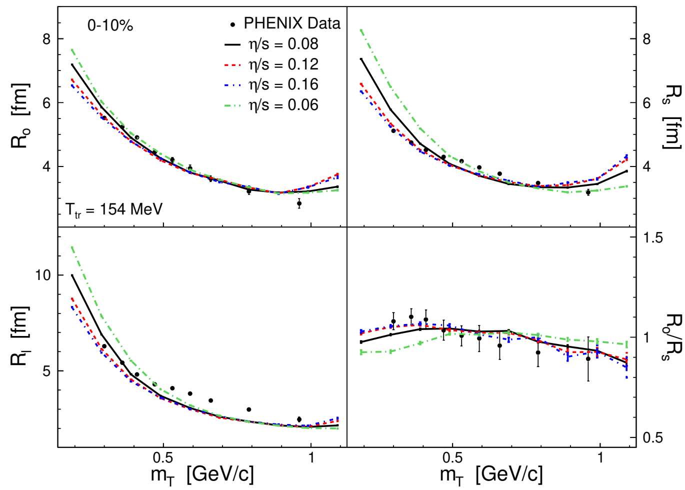

Fig. 3. HBT radii of charged pions with various η/s at $T_{\text{tr}} = 154$ MeV.

AMPT model, generating heavy-ion collision events that only include pions directly produced from hadronization. Figures 4 and 5 show the charged pion HBT radii without ω decays as a function of the average transverse mass for Au+Au collisions. It can be observed from the figures that resonance decays only affect the size of the HBT radius in the small-m_{T} range and do not change the trend of the dependence of the HBT radius on m_{T} with respect to T_{tr} and η/s, indicating that the changes in T_{tr} and η/s can be reflected in the evolution of the collision system through the HBT radius.

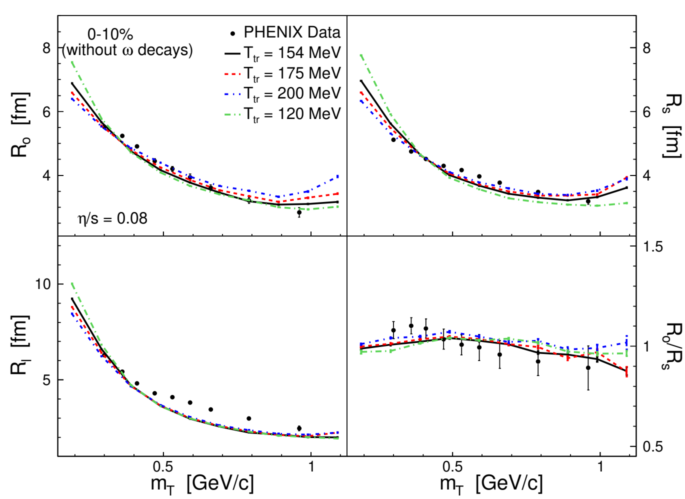

Fig. 4. The same as Fig. 1 but without ω decays.

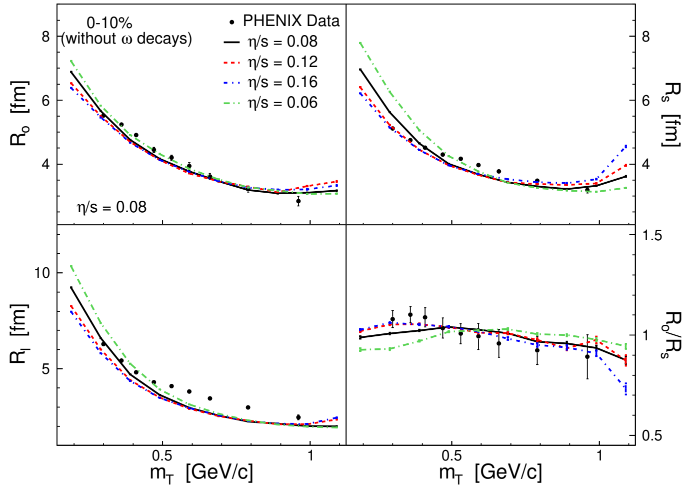

Fig. 5. The same as Fig. 3 but without ω decays.

Figure 6 shows the transverse flow velocity of charged pions as a function of the transverse mass for Au+Au collisions at $\sqrt{s_{NN}} = 200$ GeV in 0–10% centrality, where the left figures present $m_{\rm T} - m_0 = [0, 0.2]$ GeV/c^2, the right figures $m_{\rm T} - m_0 = [0.2, 1.0]$ GeV/c^2. It is noteworthy that the influence trends of $T_{\rm tr}$ and η/s on transverse flow velocity $\beta_{\rm T}$ with $m_{\rm T}$ variation

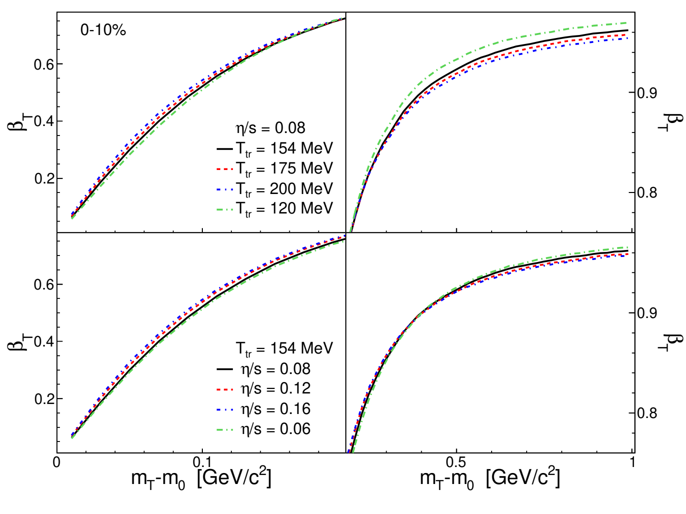

Fig. 6. Transverse flow velocity of charged pions varies with the transverse mass for Au+Au collisions at $\sqrt{s_{NN}} = 200$ GeV in 0–10% centrality. Top: constant η/s. Bottom: constant $T_{\rm tr}$.

are consistent with the trends of HBT radius dependence on $m_{\rm T}$, and the range of $m_{\rm T}$ affected is also consistent, indicating that $T_{\rm tr}$ and η/s affect the transverse flow velocity in the system evolution process, and the changes in $\beta_{\rm T}$ lead to differences in the transverse-mass dependence of the HBT radius.

For constant η/s, the increase in $T_{\rm tr}$ enhances $\beta_{\rm T}$ in the small-$m_{\rm T}$ range and suppresses it in the large-$m_{\rm T}$ range. This results in particles with increased $\beta_{\rm T}$ in the small-$m_{\rm T}$ range emitting earlier from the source with a reduced transverse radius, while those in the large-$m_{\rm T}$ range with decreased $\beta_{\rm T}$ emit later with an increased transverse radius, and $\beta_{\rm T}$ has a smaller effect on longitudinal expansion. The main reason for $\beta_{\rm T}$ to be affected by the phase-transition temperature is that a higher $T_{\rm tr}$ shortens the evolution time of the parton phase, thereby extending the evolution duration of the hadron phase. The shear viscosity in the hadronic-transport process is much greater than in the partonic-transport process. The stronger hadron phase viscosity suppresses the outward movement of large transverse-mass particles while promoting the movement of small transverse-mass particles. The longer the hadron phase duration, the greater the impact on particle movement. The transverse HBT radius dependence on transverse mass is mainly influenced by $T_{\rm tr}$ due to changes in the duration of hadron phase evolution.

For constant $T_{\rm tr}$, shear viscosity similarly impacts transverse flow velocity. An increase in viscosity suppresses the movement of large transverse-mass particles and enhances the movement of small transverse-mass particles. However, compared to the effect of hadron phase viscosity on $\beta_{\rm T}$, the influence of parton phase viscosity is weaker, especially in the large transverse-mass range. This results in $R_{\rm o}$, which is most sensitive to transverse flow velocity, being least affected by η/s. Unlike the lower evolution temperature of the hadron phase, the evolution of the parton phase corresponds to the rapid expansion of a high-temperature system. Thus, increasing shear viscosity suppresses system expansion, reducing the system size and leading to the smaller HBT radii with greater η/s, and this is ultimately reflected in $R_{\rm s}$ and $R_{\rm l}$, which are sensitive to system size.

The impact of the combined effects of $T_{\rm tr}$ and η/s on the system evolution is evident not only in the variations in the HBT radius size and its transverse-mass dependence but also directly affects the freeze-out temperature and evolution time scale of the pion source. The transverse-mass spectrum can be parameterized in the following exponential form as [30, 31]:

$$\frac{{\rm d}^2N}{2\pi m_{\rm T}\,{\rm d}m_{\rm T}\,{\rm d}y} = A\exp\left(-\frac{m_{\rm T}}{T}\right)\,, \tag{6}$$

where T is the inverse slope parameter and A is a normalization parameter. The freeze-out temperature T_0 is related to the parameter $T = T_0 + m\langle\beta_{\rm T}\rangle^2$ and $\langle\beta_{\rm T}\rangle$ is the average transverse flow velocity. By utilizing the dependence of the longitudinal HBT radius R_l and the corresponding T_0, the evolution time scale τ of the pion source can be extracted through the Herrmann–Bertsch formula [20]

$$R_\mathrm{l} = \tau\sqrt{\frac{T_0}{m_\mathrm{T}}\frac{K_2(m_\mathrm{T}/T_0)}{K_1(m_\mathrm{T}/T_0)}}\,, \tag{7}$$

which is derived by assuming the thermal spectrum of particles satisfied with the Cooper–Frye formula and the equilibrium thermal distribution as required by the Boltzmann approximation. m_T spectra and R_l of charged pions for Au+Au collisions at $\sqrt{s_{NN}} = 200$ GeV with $\eta/s = 0.08$ in 0–10% centrality are fitted by Eqs. (6) and (7) in Fig. 7.

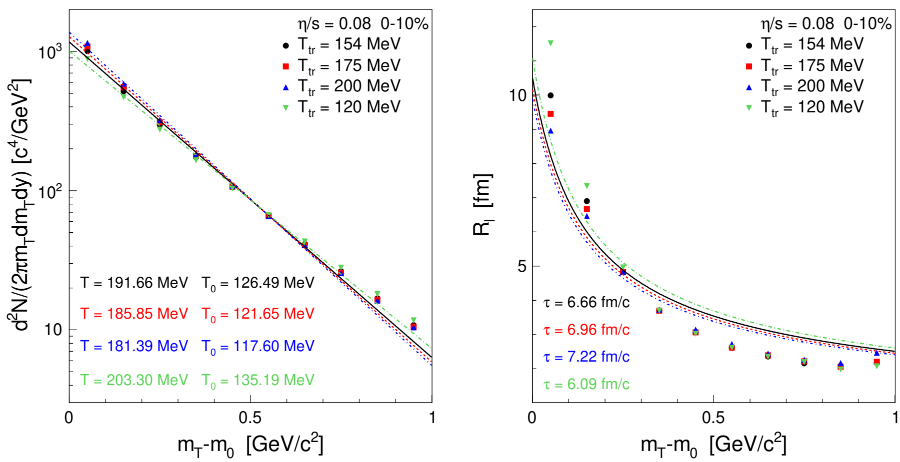

Fig. 7. Transverse-mass spectra and longitudinal HBT radii of charged pions for Au+Au collisions at $\sqrt{s_{NN}} = 200$ GeV with $\eta/s = 0.08$ in 0–10% centrality. Lines represent the fitted results using m_T exponential function (left) and the Herrmann–Bertsch formula (right), respectively.

Figure 8 shows the freeze-out temperature T_0 and evolution time scale τ of the pion source as a function of η/s for Au+Au collisions at $\sqrt{s_{NN}} = 200$ GeV in 0–10% centrality. It is evident that both η/s and T_tr significantly affect T_0 and τ. At the same shear viscosity, as phase-transition temperature increases, T_0 decreases and τ increases. This is because a higher T_tr causes the system to enter the hadron phase evolution earlier. The stronger shear viscosity in the hadron phase slows down the system expansion and evolution, resulting in a longer evolution time and a lower freeze-out temperature. For the same phase-transition temperature, as η/s increases, likewise, T_0 decreases and τ increases. Similar to the previous reason, the increase in shear viscosity slows down the system evolution. Here, the parton phase evolution is prolonged due to the increased η/s. Compared to the effect of $T_{\rm tr}$, the impact of η/s on T_0 and τ tends to saturate as η/s increases. Moreover, the higher $T_{\rm tr}$, the faster the saturation rate. This is also understandable, as a higher $T_{\rm tr}$ results in a shorter parton phase evolution time, thereby reducing the influence of η/s on parton matter. The results of T_0 and τ, like the previous HBT radii, show that $T_{\rm tr}$ and η/s directly impact the system evolution. η/s acts directly on the parton phase evolution, while $T_{\rm tr}$ regulates the duration of both the parton and hadron phase evolutions.

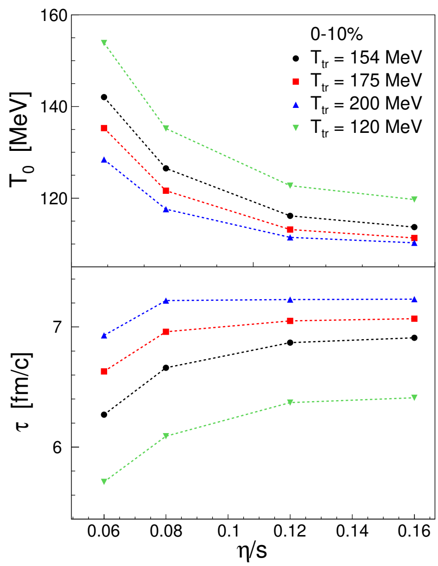

Fig. 8. Freeze-out temperature T_0 and evolution time scale τ of the pion source with various η/s at different $T_{\rm tr}$.

4. Summary

Based on the AMPT model with the shear viscous transport dynamics simulation of parton matter, we have studied the HBT radii and the evolution time scale of charged pions in the $\sqrt{s_{NN}} = 200$ GeV Au+Au collisions with various η/s and $T_{\rm tr}$. The phase-transition temperature and shear viscosity have a direct impact on the evolution process, size, and duration of both the parton and hadron phases, and this will be reflected in the final-state observables. Increasing η/s of the parton phase and raising $T_{\rm tr}$ both suppress the outward movement of high-$m_{\rm T}$ particles and enhance the movement of low-$m_{\rm T}$ particles. This leads to a reduction in transverse flow velocity in the high-m_{T} range and an increase in the low-m_{T} range, extending the evolution time scale and lowering the freeze-out temperature of the emission source. The shear viscosity η/s of the parton phase acts on the early rapid expansion process of the high-temperature and high-density system, significantly impacting the size more than the evolution time and transverse flow velocity of the system, and gives smaller values of the HBT radii. The phase-transition temperature regulates the evolution duration of the parton and hadron phases and is reflected in the evolution time scale. As T_{tr} increases, the duration of the parton phase decreases while the duration of the hadron phase increases, and the stronger viscosity in the hadronic phase greatly slows down the system evolution speed, thus extending the evolution time. However, after the rapid expansion of the high-temperature and high-density parton phase, the evolution of the hadron phase, with significantly lowered temperature and density, has a much weaker effect on the size compared to its effect on the evolution time and transverse flow velocity of the system. T_{tr} weakens the transverse-mass dependence of the transverse HBT radius, extending the evolution time scale τ. The results help in understanding the evolution of relativistic heavy-ion collisions, allowing for further study of the combined effects of T_{tr} and η/s on measured observables in data from various energy regions.

REFERENCES

[1] BRAHMS Collaboration (I. Arsene *et al.*), «Quark–gluon plasma and color glass condensate at RHIC? The perspective from the BRAHMS experiment», *Nucl. Phys. A* **757**, 1 (2005).

[2] PHOBOS Collaboration (B.B. Back *et al.*), «The PHOBOS perspective on discoveries at RHIC», *Nucl. Phys. A* **757**, 28 (2005).

[3] PHENIX Collaboration (K. Adcox *et al.*), «Formation of dense partonic matter in relativistic nucleus–nucleus collisions at RHIC: Experimental evaluation by the PHENIX Collaboration», *Nucl. Phys. A* **757**, 184 (2005).

[4] STAR Collaboration (J. Adams *et al.*), «Experimental and theoretical challenges in the search for the quark–gluon plasma: The STAR Collaboration's critical assessment of the evidence from RHIC collisions», *Nucl. Phys. A* **757**, 102 (2005).

[5] P.K. Kovtun, D.T. Son, A.O. Starinets, «Viscosity in Strongly Interacting Quantum Field Theories from Black Hole Physics», *Phys. Rev. Lett.* **94**, 111601 (2005).

[6] U. Heinz, R. Snellings, «Collective Flow and Viscosity in Relativistic Heavy-Ion Collisions», *Annu. Rev. Nucl. Part. Sci.* **63**, 123 (2013).

[7] E. Shuryak, «Strongly coupled quark–gluon plasma in heavy ion collisions», *Rev. Mod. Phys.* **89**, 035001 (2017).

[8] J.E. Bernhard, J.S. Moreland, S.A. Bass, «Bayesian estimation of the specific shear and bulk viscosity of quark–gluon plasma», *Nat. Phys.* **15**, 1113 (2019).

[9] JETSCAPE Collaboration (D. Everett *et al.*), «Phenomenological Constraints on the Transport Properties of QCD Matter with Data-Driven Model Averaging», *Phys. Rev. Lett.* **126**, 242301 (2021).

[10] J.E. Parkkila, A. Onnerstad, D.J. Kim, «Bayesian estimation of the specific shear and bulk viscosity of the quark–gluon plasma with additional flow harmonic observables», *Phys. Rev. C* **104**, 054904 (2021).

[11] Z.-W. Lin *et al.*, «Multiphase transport model for relativistic heavy ion collisions», *Phys. Rev. C* **72**, 064901 (2005).

[12] J. Xu, C.M. Ko, «Pb–Pb collisions at $\sqrt{s_{NN}} = 2.76$ TeV in a multiphase transport model», *Phys. Rev. C* **83**, 034904 (2011).

[13] G.-L. Ma, Z.-W. Lin, «Predictions for $\sqrt{s_{NN}} = 5.02$ TeV Pb+Pb collisions from a multiphase transport model», *Phys. Rev. C* **93**, 054911 (2016).

[14] T. Shao, J. Chen, C.M. Ko, Z.-W. Lin, «Enhanced production of strange baryons in high-energy nuclear collisions from a multiphase transport model», *Phys. Rev. C* **102**, 014906 (2020).

[15] Z.-W. Lin, L. Zheng, «Further developments of a multi-phase transport model for relativistic nuclear collisions», *Nucl. Sci. Tech.* **32**, 113 (2021).

[16] Y. Zhang *et al.*, «Temperature-independent shear viscosity in a multiphase transport model for relativistic heavy ion collisions», *Phys. Rev. C* **96**, 044914 (2017).

[17] Y. Zhang *et al.*, «Temperature-dependent shear viscosity in a multi-phase transport model for ultrarelativistic heavy-ion collisions at RHIC and LHC», *J. Phys. G: Nucl. Part. Phys.* **46**, 055101 (2019).

[18] Y. Zhang, Q. Liu, «Shear viscous transport dynamics simulations of parton matter in AMPT model», *Eur. Phys. J. A* **59**, 296 (2023).

[19] M.A. Lisa, S. Pratt, R. Soltz, U. Wiedemann, «Femtoscopy in Relativistic Heavy Ion Collisions: Two Decades of Progress», *Annu. Rev. Nucl. Part. Sci.* **55**, 357 (2005).

[20] STAR Collaboration (J. Adams *et al.*), «Pion interferometry in Au+Au collisions at $\sqrt{s_{NN}} = 200$ GeV», *Phys. Rev. C* **71**, 044906 (2005).

[21] STAR Collaboration (L. Adamczyk *et al.*), «Beam-energy-dependent two-pion interferometry and the freeze-out eccentricity of pions measured in heavy ion collisions at the STAR detector», *Phys. Rev. C* **92**, 014904 (2015).

[22] PHENIX Collaboration (A. Adare *et al.*), «Systematic study of charged-pion and kaon femtoscopy in Au+Au collisions at $\sqrt{s_{NN}} = 200$ GeV», *Phys. Rev. C* **92**, 034914 (2015).

[23] P. Li *et al.*, «Effects of a phase transition on two-pion interferometry in heavy ion collisions at $\sqrt{s_{NN}} = 2.4$–7.7 GeV», *Sci. China Phys. Mech. Astron.* **66**, 232011 (2023).

[24] S.-Y. Wang, J.-T. Ye, W.-N. Zhang, «Two-pion interferometry for partially coherent sources in relativistic heavy-ion collisions in a multiphase transport model», *Phys. Rev. C* **109**, 014912 (2024).

[25] N.M. MacKay, Z.-W. Lin, «The shear viscosity of parton matter under anisotropic scatterings», *Eur. Phys. J. C* **82**, 918 (2022).

[26] B. Zhang, «ZPC 1.0.1: a parton cascade for ultrarelativistic heavy ion collisions», *Comput. Phys. Commun.* **109**, 193 (1998).

[27] A. Wiranata, M. Prakash, «Shear viscosities from the Chapman–Enskog and the relaxation time approaches», *Phys. Rev. C* **85**, 054908 (2012).

[28] S. Pratt *et al.*, «Testing transport theories with correlation measurements», *Nucl. Phys. A* **566**, 103 (1994).

[29] PHENIX Collaboration (S.S. Adler *et al.*), «Bose–Einstein Correlations of Charged Pion Pairs in Au+Au Collisions at $\sqrt{s_{NN}} = 200$ GeV», *Phys. Rev. Lett.* **93**, 152302 (2004).

[30] E. Schnedermann, J. Sollfrank, U. Heinz, «Thermal phenomenology of hadrons from 200A GeV S+S collisions», *Phys. Rev. C* **48**, 2462 (1993).

[31] PHENIX Collaboration (S.S. Adler *et al.*), «Identified charged particle spectra and yields in Au+Au collisions at $\sqrt{s_{NN}} = 200$ GeV», *Phys. Rev. C* **69**, 034909 (2004).